A Comprehensive Dynamic Model for Magnetostrictive Actuators Considering Different Input Frequencies With Mechanical Loads

Zhi Li, Xiuyu Zhang, Guo-Ying Gu, *Member, IEEE*, Xinkai Chen, *Senior Member, IEEE*, and Chun-Yi Su, *Senior Member, IEEE*

***Abstract*—Magnetostrictive actuators featuring high energy densities, large strokes, and fast responses are playing an increasingly important role in micro/nano-positioning applications. However, such actuators with different input frequencies and mechanical loads exhibit complex dynamics and hysteretic behaviors, posing a great challenge on applications of the actuators. Therefore, it is important to develop a dynamic model that can characterize dynamic behaviors of the actuators, including current-magnetic flux nonlinear hysteresis, frequency responses, and loading effects, simultaneously. To this end, a comprehensive model, which thoroughly considers the electric, magnetic, and mechanical domain, as well as the interactions among them, is developed in this paper. To validate the developed model, the parameters of the model are identified where the hysteresis of the magnetostrictive actuator is described, as an illustration, by the asymmetric shifted Prandtl–Ishlinskii model. The experimental results demonstrate that the comprehensive model presents an excellent agreement with dynamic behaviors of the magnetostrictive actuator.**

***Index Terms*—Asymmetric shifted Prandtl–Ishlinskii (ASPI) model, dynamic modeling, hysteresis, magnetostrictive actuator.**

Manuscript received June 12, 2015; revised December 01, 2015 and February 10, 2016; accepted March 07, 2016. Date of publication March 15, 2016; date of current version June 02, 2016. This work was supported in part by the National Natural Science Foundation of China under Grant U1201244, Grant 61228301, and Grant 61411140039; in part by the National High-Tech Research and Development Program of China (863 Program) under Grant 2015AA042302; and in part by the Emerging Industries of Strategic Importance of Guangdong Province, China, under Grant 2012A090100012. Paper no. TII-15-0927. *(Corresponding author: Chun-Yi Su.)*

Z. Li is with the Control Systems Group, Department of Electrical Engineering, Eindhoven University of Technology, 5600 MB Eindhoven, the Netherlands.

X. Y. Zhang is with School of Automation, Northeast Dianli University, Jilin 132012, China.

G.-Y. Gu is with the State Key Laboratory of Mechanical System and Vibration, School of Mechanical Engineering, Shanghai Jiao Tong University, Shanghai 200240, China.

X. Chen is with the Department of Electronic and Information Systems, Shibaura Institute of Technology, Tokyo 337-8570, Japan.

C.-Y. Su is with the College of Mechanical Engineering and Automation, Huaqiao University, Xiamen, 361021 China, and is also on leave from Concordia University, Montreal, QC, H3G 1M8, Canada (e-mail: chun-yi.su@concordia.ca).

Color versions of one or more of the figures in this paper are available online at http://ieeexplore.ieee.org.

Digital Object Identifier 10.1109/TII.2016.2543027

I. Introduction

Magnetostrictive materials are a class of materials that change their shape when exposed to an external magnetic field. This property of the magnetostrictive materials is called magnetostriction [1] which was first discovered by James Joule in 1842. Among the available magnetostrictive materials, the giant magnetostrictive material Terfenol-D is considered the most ideal material for fabricating magnetostrictive actuators. Terfenol-D is capable of providing a positive magnetostrain of 1000–2000 ppm at 50–200 kA/m in bulk materials. In addition, Terfenol-D shows the largest room temperature magnetostriction of any known magnetostrictive material which presents a good tradeoff between high strain and high Curie temperature [2]. Featuring these properties, magnetostrictive actuators are poised to play an increasingly important role in applications of micro/nano-positioning systems [3], the high dynamic servo valve [4], hydraulic press systems [5], etc.

The input and output responses of the magnetostrictive actuator are very important index to evaluate the performance of the actuator. According to the experimental tests reported in the literature [6]–[8], the input and output responses of the magnetostrictive actuated dynamic systems associated with different input frequencies and mechanical loads show complex nonlinear effects. Such nonlinear effects will severely deteriorate the positioning and tracking performance of the actuator and meanwhile cause inaccuracy, oscillations and some other unexpected effects to the system [9]–[16], which poses a great challenge on applications of the actuator. In the literature, the input–output responses of the actuator have been thoroughly studied. However, most of them are limited to the study of only one of factors such as input frequencies [17]–[19] and applied mechanical loads [20]–[22]. In [23] and [24], although the loading effect (load range 30–700 N) is studied with different input frequencies, the experimental tests are conducted under very low input frequency (lower than 0.5 Hz), which only show the performance in very limited frequency range. To our best knowledge, there is no comprehensive study on the modeling of input–output responses of the actuator both with wide range of input frequencies and mechanical loads. This motivates us to conduct experimental tests on the input–output responses and develop a proper model to describe the corresponding responses.

In order to represent the complex dynamic behaviors, in the literature, several models have been established, which can be classified into two categories: 1) the phenomenon-based modeling approach; and 2) the physical-based modeling approach. The main idea of the phenomenon-based modeling approach is to use the input (current) and output (displacement) experimental data of the magnetostrictive actuator to do the curve fitting. For the operation of the magnetostrictive actuator in low input frequency and no mechanical loads, the input and output responses can be predicted using the hysteresis models only [25], [26]. However, these models are mainly focusing on describing the hysteresis effect in the working condition with low input frequency and without mechanical loads, and thus they fail to describe the dynamic behaviors of the actuator when the magnetostrictive actuator is operated in high input frequencies and heavy mechanical loads.

To reflect the influence of the input frequency and mechanical loads, the rate-dependent model and load-dependent model are, therefore, developed. In [27] and [28], the time derivative of model output or the time derivative of the input signal is introduced into the model to characterize the variation of the input frequency. In [23], the load term is introduced into the hysteresis model to represent the loading effect. However, these proposed models can either only describe the dynamic behavior with different input frequencies or only describe the loading effect.

Besides the phenomenon-based model mentioned above, there are also some physical-based models, which are built according to the first principles method. Among reported physical-based models, the Jiles–Atherton (J–A) model [29] is the most popular one. The J–A model developed based on the energy balance theory presents the capability of depicting the input and output responses with different input frequencies and mechanical loads. However, the limitations of the original formulation of the J–A model are unclosed minor loops [21] and quasistatic magnetomechanical behaviors [30]. To tackle these limitations, several extended J–A models were developed. However, these modifications either need prior knowledge of the input signal [31], e.g., the input extrema, or lead large model errors at high frequencies. Apart from the J–A model, the homogenized energy model [32] is also a commonly used physical-based hysteresis model and its extension [20] can describe the load-dependent hysteresis effect. However, it is not clear whether this type of model can capture the dynamic behaviors at high input frequencies.

Through the above literature analysis, we can conclude that it still requires to develop a comprehensive model, that can describe the input (current) and output (displacement) responses of the actuator with both a wide range of input frequencies and mechanical loads. In order to capture the complex input and output behaviors, current-magnetic flux hysteresis, frequency responses of the actuator, nonlinear magnetic behaviors, and the mechanical loads should be comprehensively considered in the modeling strategy. To this end, a dynamic model based on the principle of operation of the magnetostrictive actuator, which comprehensively considers the electric, magnetic, and mechanical domain as well as the interactions among them, is proposed in this paper. As will become clear later, the proposed model can be treated as an "actuator model." There is a crucial difference with respect to modeling approaches which are devoted to characterize the active material and then to predict the behavior of the actuator on the basis of the physical principles. The approach considered in this paper can serve as a base for the controller designs when the actuator has to be controlled, but it has some limits if used in the design phase of new actuators. Afterwards, to validate the developed model, the parameters of the model are identified when the hysteresis effect of the magnetostrictive actuator is represented, as an illustration, by the asymmetric shifted Prandtl–Ishlinskii (ASPI) model. Experimental validation is conducted on a magnetostrictive actuated platform. The experimental results illustrate that the comprehensive model has an excellent agreement with the dynamic behavior of the magnetostrictive actuator.

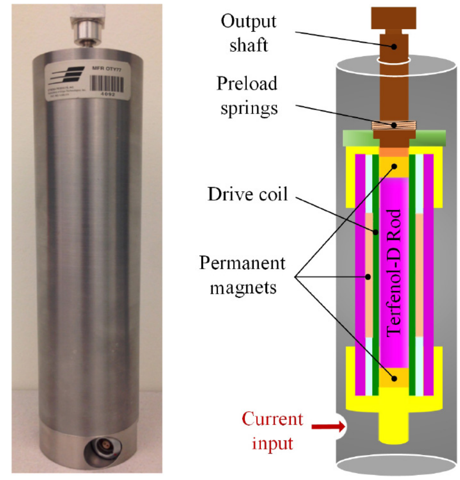

Fig. 1. Schematic illustration of the magnetostrictive actuator.

II. Dynamic Modeling of the Magnetostrictive Actuator

The magnetostrictive actuators are solid-state magnetic actuators and they convert electrical current inputs into corresponding mechanical outputs. Fig. 1 shows the inside structure of magnetostrictive actuator. From the literature reports and our experimental tests being presented later, they clearly show that the input and output responses of the magnetostrictive actuator associated with input frequencies and mechanical loads demonstrate a complex dynamic nonlinear effect. To describe this complex effect, a comprehensive modeling strategy considering the electric, magnetic, and mechanical domain inside of the actuator as well as the interactions among them is fully investigated in this section.

A. Electrical Modeling

Due to the presence of electrical-magnetic losses: hysteresis loss and eddy current loss (the definition will be given in the following development), the responses of the supplied current i and the displacement of the magnetostrictive actuator x exhibit nonlinear characteristics. Fig. 2 shows the hysteresis effect of the magnetostrictive rod. To clearly understand the mechanism of the hysteresis, the physical explanation of the hysteresis is briefly presented as follows. When a current is applied to the winding coils, a magnetic field is produced along

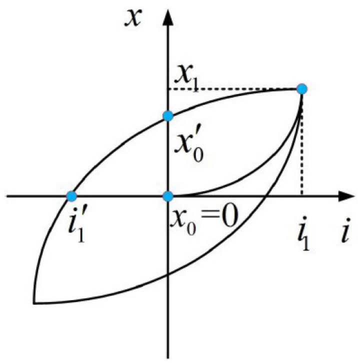

Fig. 2. Hysteresis nonlinear behavior.

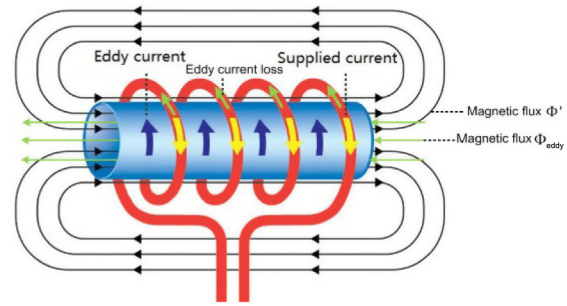

Fig. 3. Illustration of the eddy current effect.

the magnetostrictive rod, and the rod elongates at point (i_1, x_1). Then remove the supplied current, the produced magnetic field disappears immediately, while the magnetostrictive rod, point $(0, x_0')$, will not relax back exactly to zero magnetization, point (0, 0), before the current was applied. It must be driven to zero by imposing a current in the opposite direction to make the domain wall move back, point $(i_1', 0)$. Therefore, the current–displacement curve of the actuator shows a looped relationship, namely hysteresis loop. For every loop, due to this domain wall movement there will be extra work done. For this reason, there will be a consumption of electrical energy which is known as hysteresis loss of the transducer. Due to the presence of the hysteresis loss, the actual current i_a flowing through the inductance is no longer equal to the supplied current i, and one has

$$i_a = i - i_H \tag{1}$$

where i_H denotes the hysteresis loss current, which shows a nonlinear relationship with the displacement x as

$$i_H = \Pi[x] \tag{2}$$

where Π represents the hysteresis operator, which will be discussed in Section II-B.

In addition to the hysteresis loss, the actuator also has the eddy current effect. In presence of a supplied current i, a magnetic field is created, which leads to a magnetic flux Φ'. Meanwhile, according to the Faraday's law and Lenz's law, an induced electromotive force upon the rod gives rise to a current (eddy current) whose magnetic field (with a magnetic flux Φ_{eddy}) opposes the original change in magnetic flux Φ'. Then, the opposed magnetic flux Φ_{eddy} will react to the winding coils and creates an opposed current (eddy current loss) i_R, see Fig. 3.

Considering both hysteresis loss and eddy current effect, the actual current i_a flowing through the winding coils is obtained as

$$i_a = i - i_H - i_R. \tag{3}$$

Based on the Faraday's law, the eddy current loss i_R is obtained as

$$i_R = N\frac{\dot{\Phi}}{R_0} \tag{4}$$

where N is the number of coil turns, R_0 is the equivalent resistor of the eddy current effect. Φ denotes the overall magnetic flux as

$$\Phi = \Phi_L + \Phi_T \tag{5}$$

where

$$\Phi_L = i_a L_a \tag{6}$$

is the magnetic flux generated by the actual driven current, L_a denotes the equivalent inductor of the winding coils, and

$$\Phi_T = T_{\mathrm{Mm}} x \tag{7}$$

is transformed from the mechanical side which is similar to the back-emf in piezoelectric actuator [33], [34], T_{Mm} is the magnetomechanical transduction coefficient.

Substituting (2), (4), and (6) into (3), one has

$$\frac{\Phi_L}{L_a} = i - \Pi[x] - N\frac{\dot{\Phi}}{R_0}. \tag{8}$$

Then substituting (5) and (7) into (8), the complete electrical modeling expression can be written as

$$NL_a\frac{\dot{\Phi}}{R_0} + \Phi - T_{\mathrm{Mm}}x = L_a(i - \Pi[x]). \tag{9}$$

Remark: Although in (9) the relationship of the input current i and the output displacement x is established, due to the inaccessibility of the magnetic flux Φ in (9) and coupling effects from the mechanical side, the electromechanical relationship is also required, which will be established in the following development.

B. Electromechanical Modeling

According to the working principle of the magnetostrictive actuator and considering the current loss, the actually applied current should be i_a instead of i and thus the generated magnetic field H is

$$H = N_a i_a \tag{10}$$

where N_a denotes the number of turns of the solenoid per unit length. In the presence of the magnetic field H, small magnetic domains move themselves to cause internal strains in the Terfenol-D rod, leading to a force F_a as

$$F_a = AE^H d_{33} H \tag{11}$$

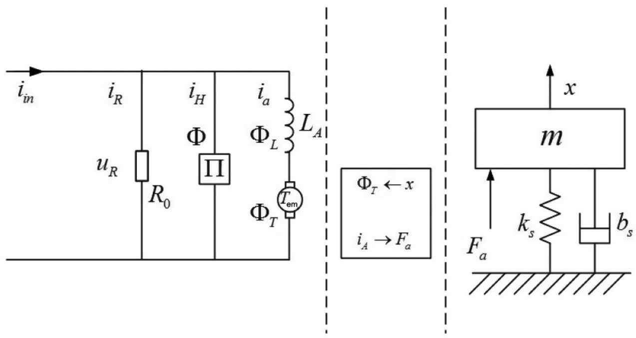

Fig. 4. Dynamic modeling of the magnetostrictive positioning system.

where A denotes the area of the magnetostrictive rod, E^H denotes the Young's modulus at constant value of magnetic field H, d_{33} is the slope of the strain versus magnetic field. Substituting (10) into (11) yields

$$F_a = AE^H d_{33} N i_a = T_{\mathrm{em}} i_a \tag{12}$$

where $T_{\mathrm{em}} = AE^H d_{33} N$ denotes the electromechanical transduction coefficient. Since we only interest in the endpoint displacement of the actuator, the mechanical dynamic (force–displacement) responses of magnetostrictive actuator can be simplified as a mass–spring–damper system, which is defined as

$$m\ddot{x} + b_s \dot{x} + k_s x = F_a \tag{13}$$

where x denotes the endpoint displacement of the actuator, m is the mass of the moving part with $m = m_0 + m_l$, where m_0 denotes the mass of the output shaft without mechanical loads and m_l denotes the applied mechanical loads, b_s is the damping coefficient, and k_s is the stiffness.

Substituting (5)–(7), and (12) into (13), the electromechanical relationship can be formulated as

$$m\ddot{x}(t) + b_s \dot{x}(t) + \left(k_s + \frac{T_{\mathrm{em}} T_{\mathrm{Mm}}}{L_a}\right) x(t) = \frac{T_{\mathrm{em}}}{L_a}\Phi. \tag{14}$$

C. Development of the Comprehensive Dynamic Model

The developed comprehensive dynamic model, including the electrical modeling (9) and the electromechanical modeling (14), can be expressed as follows:

$$m\ddot{x}(t) + b_s \dot{x}(t) + \left(k_s + \frac{T_{\mathrm{em}} T_{\mathrm{Mm}}}{L_a}\right) x(t) = \frac{T_{\mathrm{em}}}{L_a}\Phi \tag{15}$$

$$N L_a \frac{\dot{\Phi}}{R_0} + \Phi - T_{\mathrm{Mm}} x = L_a (i - \Pi[x]). \tag{16}$$

Fig. 4 illustrates the comprehensive dynamic model of the magnetostrictive actuator resulting from the aforementioned analysis.

Remarks: A complete comprehensive model of the magnetostrictive positioning system proposed in (15) and (16) accounts for both hysteresis nonlinear effects and dynamics in the magnetostrictive positioning systems. Surprisingly, until now there is no such a complete description available in the literature although some papers have addressed this issue [6]–[37]. It might be the case that most of available results only focused on a magnetostrictive actuator itself without considering the loads as a whole system. For instance, in the previous work [36], a dynamic model consisting of a second-order linear plant with hysteresis nonlinearities was developed to describe the behaviors of the magnetostrictive actuator. However, the equivalent resistor of the eddy current effect R_0 in Fig. 4 was not considered which results in an incomplete description in electrical modeling. The proposed model in this paper can be reduced to this special case if the equivalent resistor R_0 becomes infinity in (16). In [37], a linear modeling approach is proposed for describing the magnetostrictive actuated system, where the hysteresis effect of the magnetostrictive actuator is ignored. The proposed model can also be reduced to this case without considering the hysteresis effect $\Pi[x]$ in (16).

It is well known that dynamic model of a permanent magnet dc motor can be described as

$$L_m \frac{di_m(t)}{dt} + R_m i_m(t) + K_{\mathrm{emf}} \frac{d\theta(t)}{dt} = v_{in}(t) \tag{17}$$

$$J\ddot{\theta}(t) + B\dot{\theta}(t) = K_t i_m(t) \tag{18}$$

where $i_m(t)$ is the armature current, $\theta(t)$ is the angular position, L_m, R_m, K_{emf}, and K_t are the inductance, resistance, back-emf constant, and torque constant of the motor, respectively. J is the inertia of the rotor and the equivalent mechanical load, and B is the damping coefficient. From (15) and (16), we can find that the dynamic model of the magnetostrictive positioning platform is very similar to the traditional dc motor (17) and (18) except the hysteresis nonlinearity $\Pi[x]$. Therefore, the challenge for control of the magnetostrictive positioning platform system mainly lies in accommodating the nonsmooth nonlinear hysteresis $\Pi[x]$, which usually deteriorates the system performance in such manners as generating undesirable inaccuracies or oscillations.

The proposed models (15) and (16) involve many unknown parameters. Some of them could be even nonlinear or not constant. It is very difficult, if not impossible, to get their values. As will be illustrated in Section III, the parameters of the model are generally identified based on the input and output signals. The identified parameters are usually not exact, containing some errors possibly due to the changes of some parameters. However, tolerance of the model error depends on applications. We should emphasize the purpose of proposing such a model is possibility to develop a general control framework including the robust and adaptive control schemes, which can count for the unknown and changes of the system parameters.

III. Experimental Evaluation

A. Experimental Platform

The experimental tests were conducted on a magnetostrictive actuator MFR OTY77, manufactured by Etrema Products, Inc. A capacitive sensor (Lion Precision, model C23-C250) with a capacitive sensor driver (Lion Precision, Elite Series CPL190) was used for measurement of the actuator displacement response with a sensitivity of 80 mV/μm. The excitation

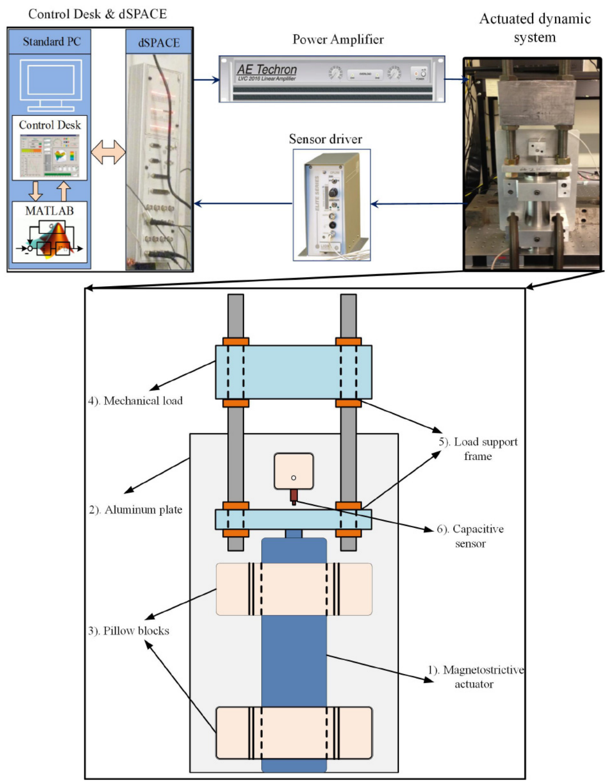

Fig. 5. Experimental platform.

TABLE I
COEFFICIENTS OF THE ASPI MODEL

Numbers	r_i	p_i	c_i	q_i	a_i
0	0	0.9002			0
1	0.3	0.8445	1.1	1.3809	0
2	0.6	0.4276	1.2	0	0.3106
3	0.9	1.4821	1.3	0	0.0417
4	1.2	0.6097	1.4	0	
5	1.5	1.3596	1.5	0	
6	1.8	1.2051	1.6	0	
7	2.1	1.0574	1.7	0	
8	2.4	0.2835	1.8	1.0056	
9	2.7	0.1636			

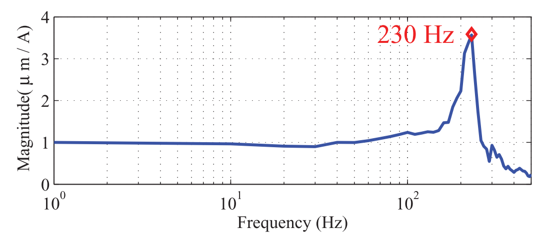

Fig. 6. Frequency response of the system.

current to the actuator was applied through the power amplifier LVC2016 produced by AE Techron Inc. The displacement response of the actuator, measured by the capacitive sensor, was obtained via the dSPACE control board equipped with 16-bit analog-to-digital converters (ADCs) and 16-bit digital-to-analog converters (DACs). We should mention that a preload has been applied to the magnetostrictive rod using a spring by the manufacturers. In our experiments, we take this preload as the reference point and all the measurements are based on this reference point. Fig. 5 illustrates the whole experimental platform, with a 156.8-N load.

From (15) and (16), one has

$$\dddot{x} + \rho_2 \ddot{x} + \rho_1 \dot{x} + \rho_0 x = b(i - \Pi[\Phi]) \tag{19}$$

where $\rho_2 = \frac{NL_a b_s + R_0 m}{NL_a m}$, $\rho_1 = \frac{NL_a k_s + NT_{\mathrm{em}} T_{\mathrm{Mm}} + R_0 b_s}{NL_a m}$, $\rho_0 = \frac{k_s R_0}{NL_a m}$, $b = \frac{R_0 T_{\mathrm{em}}}{NL_a m}$. Because the induced magnetic flux $\Phi(t)$ in the circuit can be represented as a function of supplied current $i(t)$, i.e., $\Phi(t) = \zeta(i(t))$, the term $i - \Pi[\zeta[i]]$ in (19) can be defined as a new hysteresis nonlinearity $\Gamma[i](t)$

$$\Gamma[i](t) = u(t) = i(t) - \Pi[\Phi](t). \tag{20}$$

The model of the magnetostrictive actuated system can be rewritten as

$$\dddot{x} + \rho_2 \ddot{x} + \rho_1 \dot{x} + \rho_0 x = b\Gamma[i](t). \tag{21}$$

B. Hysteresis Modeling

In this section, the hysteresis operator $\Gamma[i](t)$ defined in (21) will be specified as an illustration. In the literature, many hysteresis models have been proposed for representing hysteresis behaviors, such as Preisach model [38], J–A model [29], Prandtl–Ishlinskii (PI) model [39], Bouc–Wen model [40], and Duhem model [41]. As an illustration, an extended PI model, the ASPI model [42], is utilized in this paper to describe the asymmetric hysteresis behavior in the magnetostrictive actuator. It is noted that the selection of the hysteresis model is open and interested readers may refer to [43] and [44] for different asymmetric hysteresis models.

The ASPI model is defined as

$$u(t) = \Gamma[i](t) = P[i](t) + \Psi[i](t) + g(i)(t) \tag{22}$$

where the first term $P[i](t)$ is the PI model [45], which is defined as

$$P[i](t) = p_0 i(t) + \int_0^\infty p(r) F_r[i](t) dr \tag{23}$$

where p_0 is a positive constant; $p(r)$ is a given density function, satisfying $p(r) \geq 0$ with $\int_0^\infty r p(r) dr < \infty$; $F_r[i]$ is the play operator with a threshold r

$$F_r[i](0) = f_r(i(0), 0) \tag{24}$$

$$F_r[i](t) = f_r(i(t), F_r[i](t_j)) \tag{25}$$

for $t_j < t \leq t_{j+1}, 0 \leq j \leq N-1$, with

$$f_r(i, w) = \max(i - r, \min(i + r, w)) \tag{26}$$

where $0 = t_0 < t_1 < \cdots < t_N = t_E$ is a partition of $[0, t_E]$, such that the function $i(t)$ is monotone on each of the subintervals $[t_j, t_{j+1}]$. The second term $\Psi[i](t)$ in (22) is the shifted model, which is written as

$$\Psi[i](t) = \int_{c_0}^{c_1} \chi(c) \Psi_c[i](t) dc \tag{27}$$

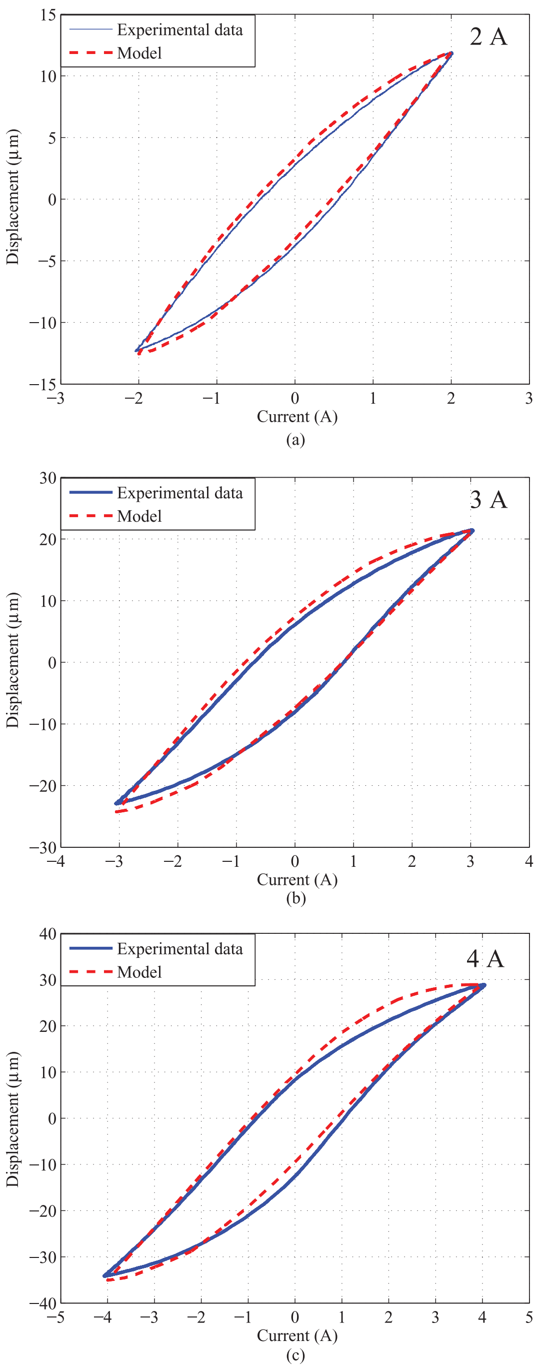

Fig. 7. Model validation with different input amplitudes and no mechanical loads. (a) Comparison of the experimental data and dynamic model with sinusoidal input $2\sin(2\pi t)$. (b) Comparison of the experimental data and dynamic model with sinusoidal input $3\sin(2\pi t)$. (c) Comparison of the experimental data and dynamic model with sinusoidal input $4\sin(2\pi t)$.

where $\chi(c)$ is the density function satisfying $\chi(c) \geq 0$, $\Psi_c[i](t)$ is the shift operator defined as

$$\Psi_c[i](0) = \psi_c(i(0), 0) \tag{28}$$

$$\Psi_c[i](t) = \psi_c(i(t), \psi_c[i](t_j)) \tag{29}$$

for $t_j < t \leq t_{j+1}, 0 \leq j \leq N-1$, with

$$\psi_c(i, w) = \max(ci, \min(i, w)) \tag{30}$$

TABLE II
MODELING ERROR WITH DIFFERENT INPUT AMPLITUDES

Amplitudes (A)	2	3	4
MME (%)	3.44	3.67	5.72

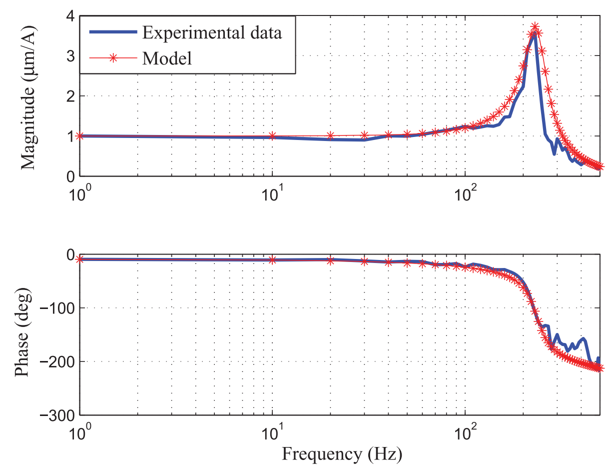

Fig. 8. Comparison of the frequency response of the system and the dynamic model with a mechanical load 156.8 N.

where $0 = t_0 < t_1 < \ldots < t_N$ is the partition of $[0, t_N]$. $c \in \mathbb{R}_+$, $\mathbb{R}_+ := \{x \in \mathbb{R} | x \geq 0\}$ is a parameter to determine the shape of the shift operator. When $c > 1$, $\Psi_c[i](t)$ is called left shift operator; when $0 < c < 1$, $\Psi_c[i](t)$ is called right shift operator. The last term $g(i)(t)$ in (22) is a Lipschitz continuous and derivative function, which assists to represent the saturation behavior of hysteresis nonlinearity.

C. Model Identification

In this section, the parameters of the dynamic model in (21) will be estimated in two steps. Step 1) Identification of the hysteresis part. In order to facilitate the model parameters identification, we have the discrete form of the ASPI model as

$$\begin{aligned} u(t) &= P[i](t) + \Psi[i](t) + g(i)(t) \\ &= p_0 i(t) + \sum_{j=1}^{n} p_j F_{r_j}[i](t) \\ &\quad + \sum_{j=1}^{M} q_j \Psi_{c_j}[i](t) + g(i)(t) \end{aligned} \tag{31}$$

where p_j denote the weights of the play operator; $F_{r_j}[i](t)$ are play operators at the threshold of r_j; n is the number of the play operator used for identification. q_j denote the weights of the elementary shift operators; $\Psi_{c_j}[i](t)$ are the elementary shift operators at the slope of c_j; M is the number of the elementary shift operator used for identification. $g(i)(t)$ is selected as

$$g(i)(t) = -a_3 i(t)^3 - a_2 i(t)^2 - a_1 i(t) - a_0 \tag{32}$$

n is chosen as $n = 9$, and the thresholds r_j were selected as $r_j = 0.3j$ $(j = 1, 2, \ldots, n)$. It is worth mentioning that the choice of n is a tradeoff between the modeling accuracy and computational complexity, and thereafter $n = 9$ is selected.

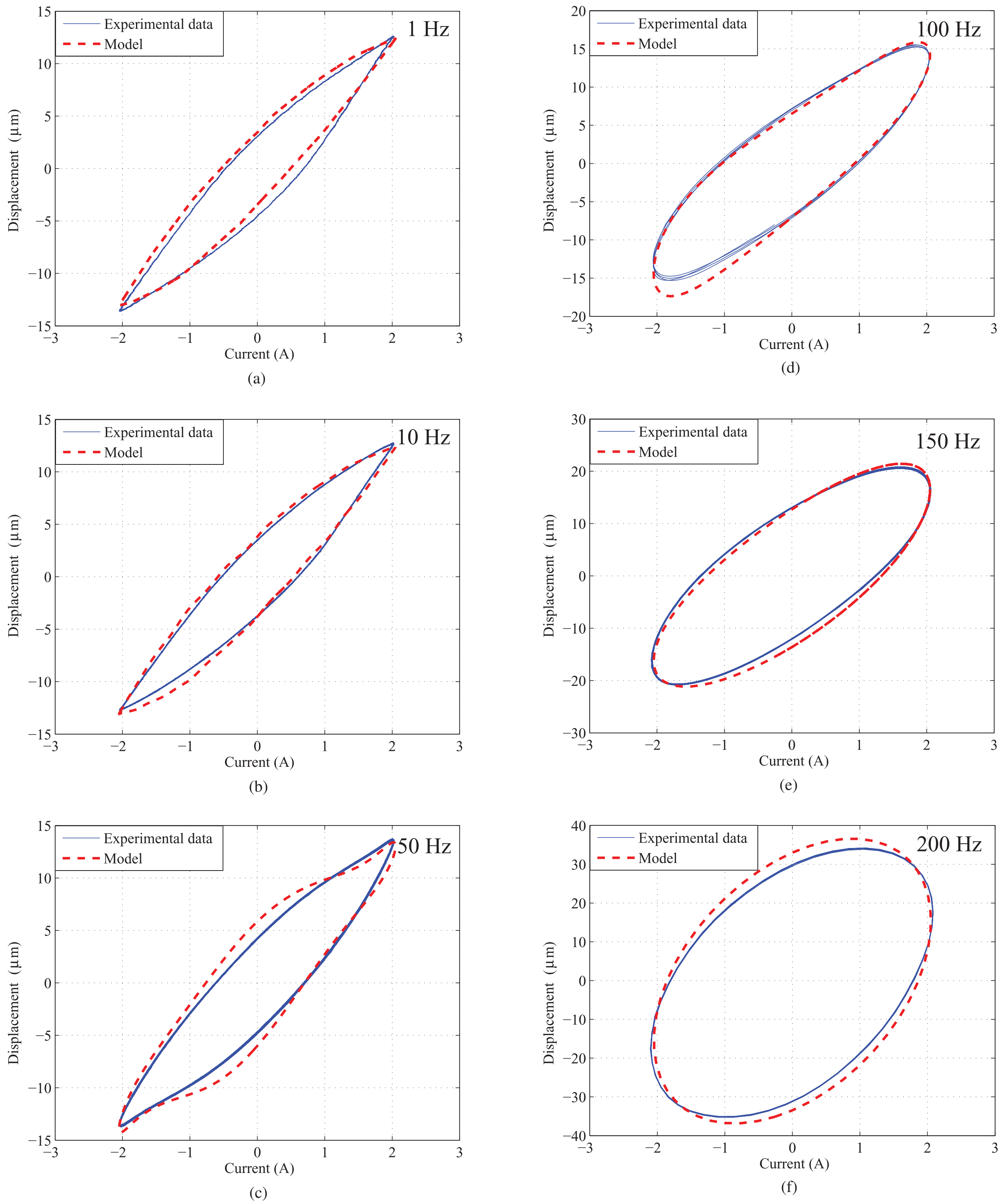

Fig. 9. Model verification with sinusoid signal under different input frequency with a mechanical load 156.8 N. (a) 1 Hz. (b) 10 Hz. (c) 50 Hz. (d) 100 Hz. (e) 150 Hz. (f) 200 Hz.

Table I shows the identified parameters. Step 2) Identification of the dynamic part. We first decompose $G_1(s)$ as

$$G_1(s) = \frac{\tau}{s+\tau} \cdot \frac{\omega_n^2}{s^2 + 2\xi\omega_n s + \omega_n^2} \tag{33}$$

with $\rho_2 = 2\xi\omega_n + \tau$, $\rho_1 = \omega_n^2 + 2\xi\omega_n\tau$, $\rho_0 = \tau\omega_n^2$. The objective is to identify the parameters of τ, ξ, ω_n. To this end, a frequency response (1–500 Hz) of the magnetostrictive actuator is obtained in Fig. 6, where the applied mechanical load is 156.8 N.

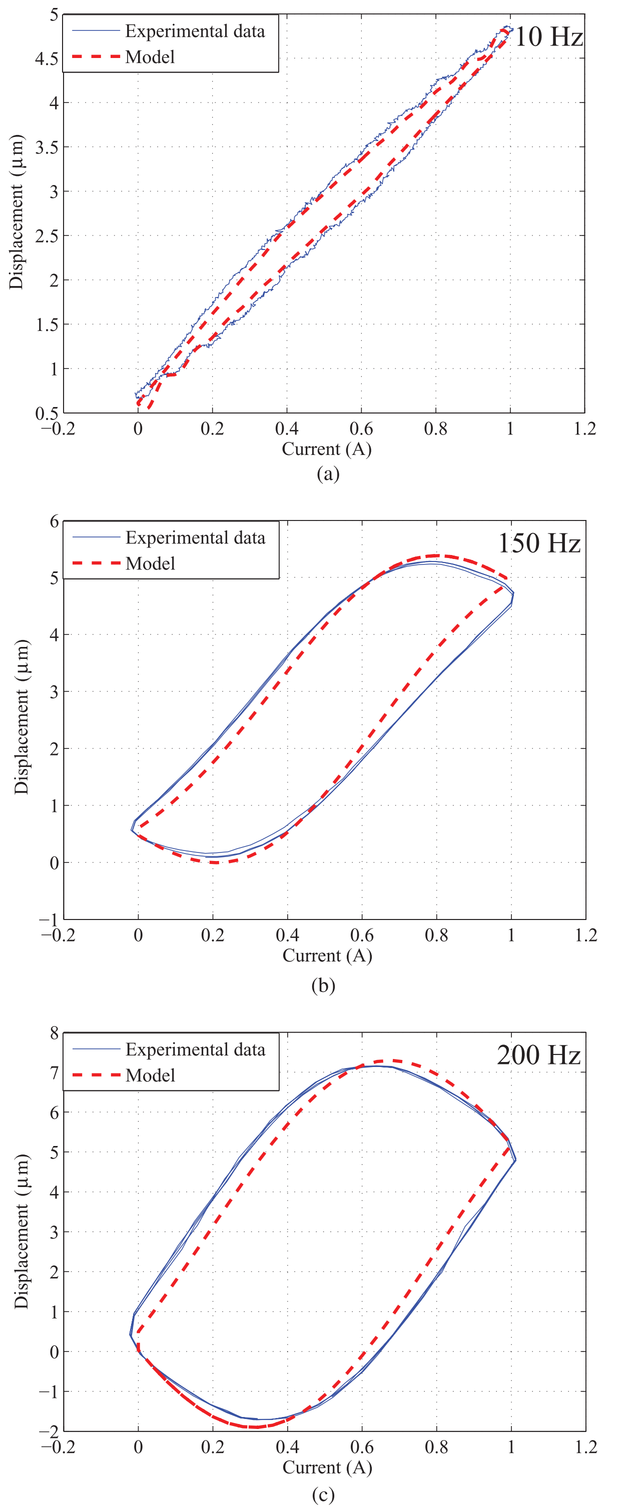

Fig. 10. Model verification with triangular signal under different input frequency with a mechanical load 156.8 N. (a) 10 Hz. (b) 150 Hz. (c) 200 Hz.

From the magnitude response in Fig. 6, we can find that $\omega_n = 230 \times 2\pi$ rad/s. Then, the least square approach is utilized to identify the parameters ξ, τ as $\xi = 0.13$ and $\tau = 800 \times 2\pi$, and $G_1(s)$ is expressed as

$$G_1(s) = \frac{1.05 \times 10^{10}}{s^3 + 5402s^2 + 3.98 \times 10^6 s + 1.05 \times 10^{10}}. \quad (34)$$

TABLE III
MODELING ERROR WITH SINUSOID INPUT SIGNAL UNDER DIFFERENT FREQUENCIES

Fres. (Hz)	1	10	50	100	150	200
MME (%)	5.88	3.64	6.35	6.16	3.93	4.09

TABLE IV
MODELING ERROR WITH TRIANGULAR INPUT SIGNAL UNDER DIFFERENT FREQUENCIES

Fres. (Hz)	10	150	200
MME (%)	3.59	9.72	6.60

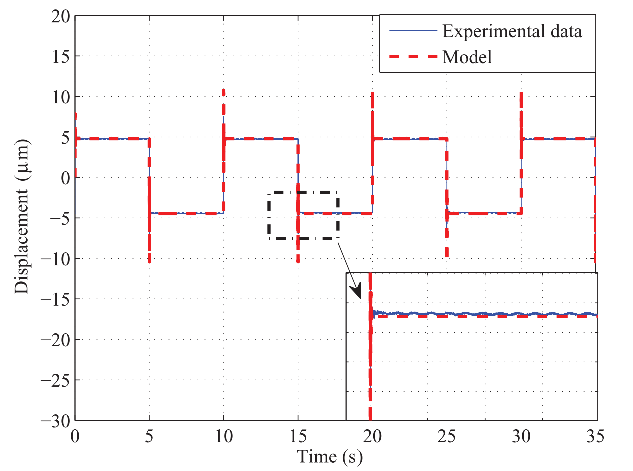

Fig. 11. Model verification with square wave with a mechanical load 156.8 N.

D. Model Validation

1) Model Validation With Different Input Amplitudes in Low Input Frequencies Without a Mechanical Load: We first verify the dynamic model with the operation of the magnetostrictive actuator in low frequency. The applied currents are sinusoidal currents $i_{\text{app}}(t) = I\sin(2\pi t)$ with $(I = 2, 3, 4)$. The resulting input–output responses are illustrated in Fig. 7(a)–(c). To examine the accuracy of the dynamic model, the maximum modeling error (MME) is defined as

$$e_m(t) = \frac{\max(|x_e(t) - x(t)|)}{\max(x(t)) - \min(x(t))} \times 100\% \quad (35)$$

where $x_e(t)$ and $x(t)$ denote the output of the magnetostrictive actuator and the dynamic model. Table II demonstrates the resulting MME for different input amplitudes. It can be concluded that the dynamic model shows a fairly good agreement with the experimental data in low input frequencies.

2) Model Validation in Different Input Frequencies With a Mechanical Load: To validate the dynamic characteristics of the proposed model, different input frequencies with a specified mechanical load (156.8 N) is applied to conduct the test. Fig. 8 shows the comparison of the frequency responses between the experimental data and the developed model. From the comparison, it suggests that the model can capture the main characteristics of the frequency responses of

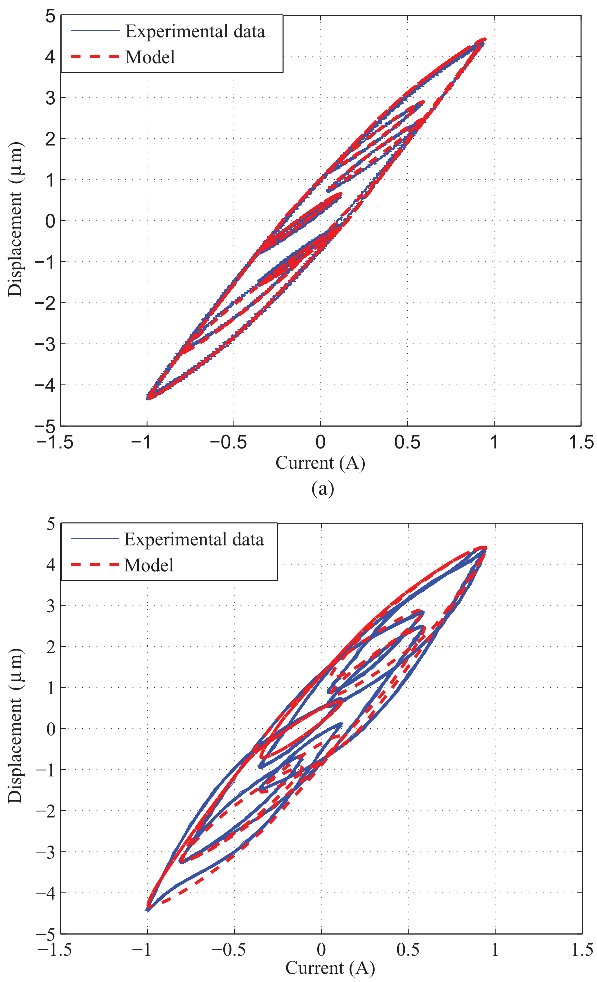

Fig. 12. Model validation with complex harmonic input with a mechanical load 156.8 N. (a) $f_0 = 1$. (b) $f_0 = 401$.

the magnetostrictive actuated dynamic system. Fig. 9 and 10 demonstrate the comparisons of the experimental data and the model with the sinusoid input signal under different frequencies (1, 10, 50, 100, 150, and 200 Hz) and with triangular input signal under different frequencies (10, 150, and 200 Hz). Tables III and IV illustrate the modeling error. They suggest that the MME under the mechanical load 156.8 N is not increasing with the increase of the input frequency. For example, for the sinusoid input case, the MME in 200 Hz is 4.09% which is smaller than that in 50 Hz. It is also true for the triangular input case. To validate the transient responses of the model, a square wave is also applied to the actuator, see Fig. 11. Moreover, a harmonic input $y = 0.44\sin(0.35 \times 2\pi f_0 t) + 0.55\sin(0.1 \times 2\pi f_0 t + \frac{\pi}{2} f_0)$ $(f_0 = 1401)$ is also applied to verify the model under complex input signal, see Fig. 12. From the figures, it can be seen that the developed model shows a good performance to describe the minor loops in the hysteresis effect and the minor loops are also closed.

3) Model Validation in Different Input Frequencies With Different Mechanical Loads: In this section, different mechanical loads and different input frequencies are also applied to validate the model. Because some parameters are

TABLE V
COEFFICIENTS OF DYNAMIC MODEL WITH DIFFERENT MECHANICAL LOADS

Loads	ρ_2	ρ_1	ρ_0
41.2N	2.256×10^4	1.799×10^7	1.221×10^{11}
98.0N	1.054×10^4	8.585×10^6	3.692×10^{10}
269.5N	1.240×10^4	8.301×10^6	2.416×10^{10}

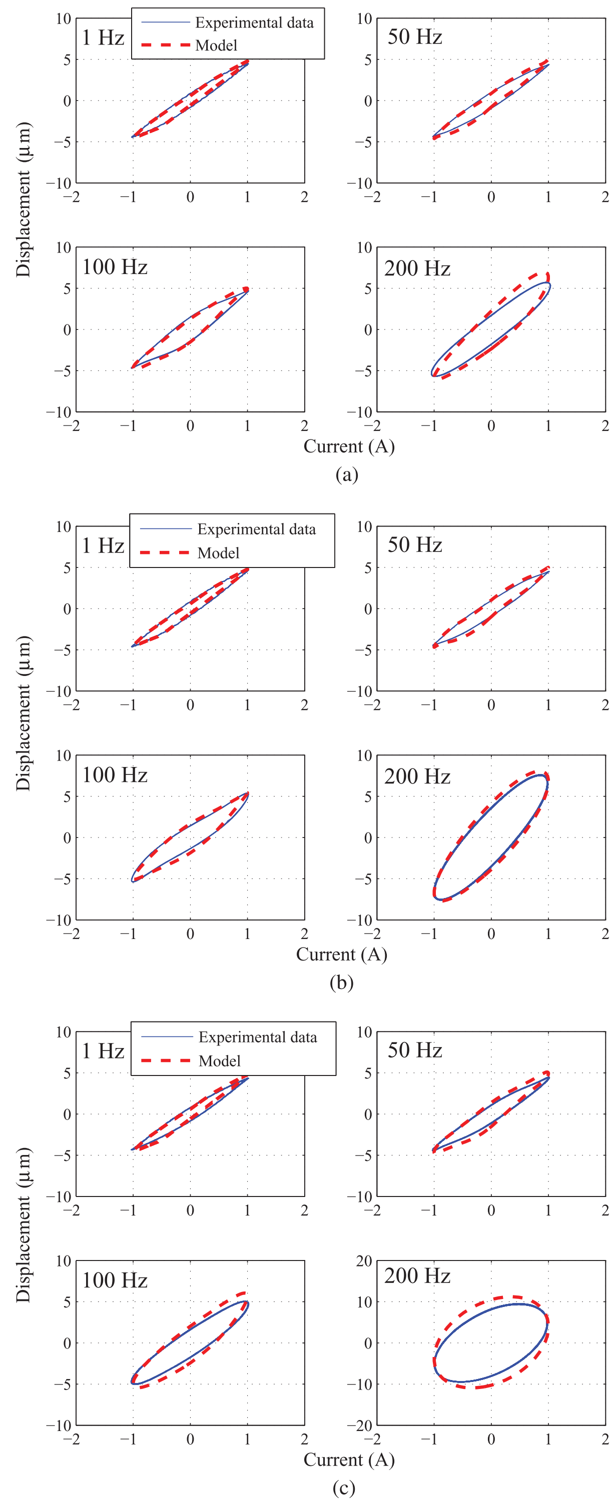

Fig. 13. Model verification in different input frequencies with different mechanical loads. (a) 41.2 N. (b) 98.0 N. (c) 269.5 N.

TABLE VI
MODELING ERROR WITH DIFFERENT FREQUENCIES AND MECHANICAL LOADS

Fres.	41.2N	98.0N	269.5N
1 Hz	4.34%	4.18%	6.17%
50 Hz	6.13%	5.80%	7.40%
100 Hz	5.92%	7.90%	10.65%
200 Hz	9.90%	3.00%	9.66%

not accessible so far, such as the electromechanical transduction coefficient T_{em} in (12), when changing the mechanical loads, the parameters in the dynamic part in (19) need to be re-identified following the Step 2 reported in Section III-C. It is also noted that the parameters in the hysteresis model under different mechanical loads remain the same, as the hysteresis current loss is regarded as a static component in the proposed comprehensive model. Table V shows the identified parameters ρ_2, ρ_1, and ρ_0 with different mechanical loads 41.2, 98.0, and 269.5 N. Fig. 13 shows the comparison of the experimental data and the dynamic model with different input frequencies in sinusoid inputs (1, 50, 100, and 200 Hz) and different mechanical loads. Table VI shows the MME under these supplies. Expect for the supply input frequency 100 Hz and mechanical load 269.5 N, the MME is within 10%. It also indicates that with heavier mechanical loads, the MME will become larger. We should mention that the verification of the model with different mechanical loads needs to re-identify the parameter changes to show the validity of the developed model. However, the purpose of proposing such a model is possibility to develop a general control framework including the robust and adaptive control schemes with unknown or changes of the parameters.

IV. CONCLUSION

In this paper, a comprehensive dynamic model considering both the nonlinear hysteresis effect and the dynamic behaviors is proposed. The developed model is based on the working principle of the magnetostrictive actuator, which comprehensively considers the electric, magnetic, and mechanical domain as well as the interactions among them. To validate the proposed model, the ASPI model is adopted as an illustration to describe the asymmetric hysteresis phenomenon. After the determination of the hysteresis model, the parameters identification of the developed comprehensive model and experimental verification are conducted in which different input signals with different input frequencies are applied to magnetostrictive actuators. The experimental results suggest that the comprehensive model has a good agreement with the dynamic and hysteresis behavior of the magnetostrictive actuator. In particularly, the proposed model can be thought of as an initial step toward the development of a general control framework. Depending on applications, it also provides a base for various controller designs.

REFERENCES

[1] D. Davino, A. Giustiniani, and C. Visone, “A two-port nonlinear model for magnetoelastic energy-harvesting devices,” *IEEE Trans. Ind. Electron.*, vol. 58, no. 6, pp. 2556–2564, Jun. 2011.

[2] A. G. Olabi and A. Grunwald, “Design and application of magnetostrictive materials,” *Mater. Des.*, vol. 29, no. 2, pp. 469–483, 2008.

[3] Q. Xu, “Robust impedance control of a compliant microgripper for high-speed position/force regulation,” *IEEE Trans. Ind. Electron.*, vol. 62, no. 2, pp. 1201–1209, Feb. 2015.

[4] Z. Yang, Z. He, D. Li, J. Yu, X. Cui, and Z. Zhao, “Direct drive servo valve based on magnetostrictive actuator: Multi-coupled modeling and its compound control strategy,” *Sensor Actuators A, Phys.*, vol. 235, pp. 119–130, 2015.

[5] X. Lu, B. Fan, and M. Huang, “A novel LS-SVM modeling method for a hydraulic press forging process with multiple localized solutions,” *IEEE Trans. Ind. Informat.*, vol. 11, no. 3, pp. 663–670, Jun. 2015.

[6] X. B. Tan and J. S. Baras, “Modeling and control of hysteresis in magnetostrictive actuators,” *Automatica*, vol. 40, no. 9, pp. 1469–1480, 2004.

[7] L. Li, C. Zhang, B. Yan, L. Zhang, and X. Li, “Research of fast-response giant magnetostrictive actuator for space propulsion system,” *IEEE Trans. Plasma Sci.*, vol. 39, no. 2, pp. 744–748, Feb. 2011.

[8] W. S. Oates, P. G. Evans, R. C. Smith, and M. J. Dapino, “Experimental implementation of a hybrid nonlinear control design for magnetostrictive actuators,” *J. Dyn. Syst. Meas. Control*, vol. 131, no. 4, p. 041004, 2009.

[9] C.-Y. Su, Q. Wang, X. Chen, and S. Rakheja, “Adaptive variable structure control of a class of nonlinear systems with unknown prandtl-ishlinskii hysteresis,” *IEEE Trans. Autom. Control*, vol. 50, no. 12, pp. 2069–2074, Dec. 2005.

[10] L. Liu, K. K. Tan, S. Chen, C. S. Teo, and T. H. Lee, “Discrete composite control of piezoelectric actuators for high-speed and precision scanning,” *IEEE Trans. Ind. Informat.*, vol. 9, no. 2, pp. 859–868, May 2013.

[11] Q. Xu, “Design and smooth position/force switching control of a miniature gripper for automated microhandling,” *IEEE Trans. Ind. Informat.*, vol. 10, no. 2, pp. 1023–1032, May 2014.

[12] J. Lee, S. Khoo, and Z.-B. Wang, “DSP-based sliding-mode control for electromagnetic-levitation precise-position system,” *IEEE Trans. Ind. Informat.*, vol. 9, no. 2, pp. 817–827, May 2013.

[13] C. Attaianese, M. Di Monaco, and G. Tomasso, “High performance digital hysteresis control for single source cascaded inverters,” *IEEE Trans. Ind. Informat.*, vol. 9, no. 2, pp. 620–629, May 2013.

[14] R. P. Aguilera, P. Lezana, and D. E. Quevedo, “Switched model predictive control for improved transient and steady-state performance,” *IEEE Trans. Ind. Informat.*, vol. 11, no. 4, pp. 968–977, Aug. 2015.

[15] G. Gu, L. Zhu, C. Y. Su, and H. Ding, “Motion control of piezoelectric positioning stages: Modeling, controller design, and experimental evaluation,” *IEEE/ASME Trans. Mechatronics*, vol. 18, no. 5, pp. 1459–1471, Oct. 2013.

[16] G. Gu, L. Zhu, C.-Y. Su, H. Ding, and S. Fatikow, “Modeling and control of piezo-actuated nanopositioning stages: A survey,” *IEEE Trans. Autom. Sci. Eng.*, vol. 13, no. 1, pp. 313–332, Jan. 2016.

[17] P. Liu, Z. Zhang, and J. Mao, “Modeling and control for giant magnetostrictive actuators with rate-dependent hysteresis,” *J. Appl. Math.*, vol. 2013, p. 8, 2013.

[18] Z. Zhang, Y. Ma, and Y. Guo, “A novel nonlinear adaptive filter for modeling of rate-dependent hysteresis in giant magnetostrictive actuators,” in *Proc. IEEE Conf. Mechatronics Autom. (ICMA)*, Beijing, China, 2015, pp. 670–675.

[19] O. Aljanaideh, S. Rakheja, and C.-Y. Su, “Experimental characterization and modeling of rate-dependent asymmetric hysteresis of magnetostrictive actuators,” *Smart Mater. Struct.*, vol. 23, no. 3, p. 035002, 2014.

[20] R. C. Smith and M. J. Dapino, “A homogenized energy model for the direct magnetomechanical effect,” *IEEE Trans. Magn.*, vol. 42, no. 8, pp. 1944–1957, Aug. 2006.

[21] V. Sina, M. Kirsten, and S. Alex, “A new load-dependent hysteresis model for magnetostrictive materials,” *Smart Mater. Struct.*, vol. 19, no. 12, p. 125003, 2010.

[22] Z. Deng and M. J. Dapino, “Characterization and finite element modeling of galfenol minor flux density loops,” *J. Intell. Mater. Syst. Struct.*, vol. 26, no. 1, pp. 47–55, 2015.

[23] D. Davino, A. Giustiniani, and C. Visone, “Experimental properties of an efficient stress-dependent magnetostriction model,” *J. Appl. Phys.*, vol. 105, no. 7, pp. 105–107, 2009.

[24] Y.-H. Ma and J.-Q. Mao, “On modeling and tracking control for a smart structure with stress-dependent hysteresis nonlinearity,” *Acta Autom. Sin.*, vol. 36, no. 11, pp. 1611–1619, 2010.

[25] Z. Li, C.-Y. Su, and T. Chai, “Compensation of hysteresis nonlinearity in magnetostrictive actuators with inverse multiplicative structure for preisach model,” *IEEE Trans. Autom. Sci. Eng.*, vol. 11, no. 2, pp. 613–619, Apr. 2014.

[26] C. Natale, F. Velardi, and C. Visone, "Identification and compensation of preisach hysteresis models for magnetostrictive actuators," *Phys. B Condens. Matter*, vol. 306, no. 1, pp. 161–165, 2001.
[27] I. D. Mayergoyz, "Dynamic preisach models of hysteresis," *IEEE Trans. Magn.*, vol. 24, no. 6, pp. 2925–2927, Nov. 1988.
[28] R. B. Mrad and H. Hu, "A model for voltage-to-displacement dynamics in piezoceramic actuators subject to dynamic-voltage excitations," *IEEE/ASME Trans. Mechatronics*, vol. 7, no. 4, pp. 479–489, Dec. 2002.
[29] D. C. Jiles and D. L. Atherton, "Theory of ferromagnetic hysteresis," *J. Magn. Magn. Mater.*, vol. 61, nos.1–2, pp. 48–60, 1986.
[30] K. Jin, Y. Kou, Y. Liang, and X. Zheng, "Effects of hysteresis losses on dynamic behavior of magnetostrictive actuators," *J. Appl. Phys.*, vol. 110, no. 9, p. 093908, 2011.
[31] D. C. Jiles, "A self consistent generalized model for the calculation of minor loop excursions in the theory of hysteresis," *IEEE Trans. Magn.*, vol. 28, no. 5, pp. 2602–2604, Sep. 1992.
[32] R. C. Smith, M. J. Dapino, and S. Seelecke, "Free energy model for hysteresis in magnetostrictive transducers," *J. Appl. Phys.*, vol. 93, no. 1, pp. 458–466, 2003.
[33] H. Adriaens, W. Koning, and R. Banning, "Modeling piezoelectric actuators," *IEEE/ASME Trans. Mechatronics*, vol. 5, no. 4, pp. 331–341, Dec. 2000.
[34] G. Gu, L. Zhu, and C.-Y. Su, "Modeling and compensation of asymmetric hysteresis nonlinearity for piezoceramic actuators with a modified prandtl-ishlinskii model," *IEEE Trans. Ind. Electron.*, vol. 61, no. 3, pp. 1583–1595, Mar. 2014.
[35] D. Davino, C. Natale, S. Pirozzi, and C. Visone, "Phenomenological dynamic model of a magnetostrictive actuator," *Phys. B Condens. Matter*, vol. 343, no. 1, pp. 112–116, 2004.
[36] G. Gu, Z. Li, L. Zhu, and C.-Y. Su, "A comprehensive dynamic modeling approach for giant magnetostrictive material actuators," *Smart Mater. Struct.*, vol. 22, no. 12, p. 125005, 2013.
[37] F. Braghin, S. Cinquemani, and F. Resta, "A model of magnetostrictive actuators for active vibration control," *Sensor Actuators A, Phys.*, vol. 165, no. 2, pp. 342–350, 2011.
[38] F. Preisach, "Über die magnetische nachwirkung," *Zeitschrift für Physik*, vol. 94, pp. 277–302, 1935.
[39] M. Brokate and J. Sprekels, *Hysteresis and Phase Transitions*. Berlin, Germany: Springer-Verlag, 1996.
[40] Y.-K. Wen, "Method for random vibration of hysteretic systems," *J. Eng. Mech. Div.*, vol. 102, no. 2, pp. 249–263, 1976.
[41] J. H. Oh and D. S. Bernstein, "Semilinear Duhem model for rate-independent and rate-dependent hysteresis," *IEEE Trans. Autom. Control*, vol. 50, no. 5, pp. 631–645, May 2005.
[42] Z. Li, C.-Y. Su, and X. Chen, "Modeling and inverse adaptive control of asymmetric hysteresis systems with applications to magnetostrictive actuator," *Control Eng. Pract.*, vol. 33, pp. 148–160, 2014.
[43] P. Ge and M. Jouaneh, "Generalized preisach model for hysteresis nonlinearity of piezoceramic actuators," *Precis. Eng.*, vol. 20, no. 2, pp. 99–111, 1997.
[44] J. Li and M. Xu, "Modified jiles-atherton-sablik model for asymmetry in magnetomechanical effect under tensile and compressive stress," *J. Appl. Phys.*, vol. 110, no. 6, p. 063918, 2011.
[45] P. Krejci and K. Kuhnen, "Inverse control of systems with hysteresis and creep," *Proc. Inst. Elect. Eng.–Control Theory Appl.*, vol. 148, no. 3, pp. 185–192, May 2001.

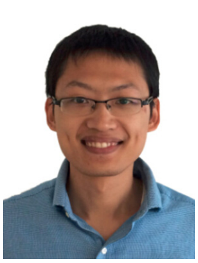

Zhi Li received the M.Sc. degree in control engineering from Northeastern University, Shenyang, China, in 2009, and the Ph.D. degree in mechanical engineering from Concordia University, Montreal, QC, Canada, in 2015.

From September 2010 to August 2011, he was a Visiting Researcher at Concordia University. Currently, he is a Post-Doctoral Research Fellow with the Department of Electrical Engineering, Eindhoven University of Technology, Eindhoven, The Netherlands. His research interests include modeling and control of the smart material-based actuators, hysteresis modeling and compensation, modeling-based battery management, and battery management systems.

Xiuyu Zhang received the B.S. degree in automation and M.S. degree in control science and engineering from Northeast Dianli University, Jilin, China, in 2003 and 2006, respectively, and the Ph.D. degree in control science and engineering from the Beijing University of Aeronautics and Astronautics (BUAA), Beijing, China, in 2012.

Currently, he is an Associate Professor with the School of Automation Engineering, Northeast Dianli University, Jilin, China. His research interests include robust and adaptive control for nonlinear systems with smart material-based actuators.

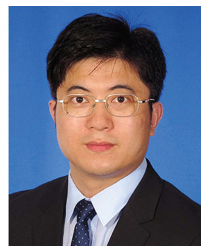

Guo-Ying Gu (S'10–M'13) received the B.E. (Hons.) degree in electronic science and technology, and the Ph.D. (Hons.) degree in mechatronic engineering from the Shanghai Jiao Tong University, Shanghai, China, in 2006 and 2012, respectively.

He was a Visiting Scholar at Concordia University, Montreal, QC, Canada, and the National University of Singapore, Singapore. Supported by the Alexander von Humboldt Foundation, he was a Humboldt Fellow with the University of Oldenburg, Oldenburg, Germany. Since October 2012, he has been with Shanghai Jiao Tong University, where he is currently appointed as an Associate Professor with the School of Mechanical Engineering. He is the author or co-author of more than 40 publications, which have published in journals, as book chapters, and in conference proceedings. His research interests include design, modeling, and control of nanopositioning stages, soft, and continuum robots.

Dr. Gu is a member of the American Society of Mechanical Engineers. Currently, he severs as the Associate Editor of the *International Journal of Advanced Robotic Systems*. He has also served for several international conferences as an Associate Editor or a Program Committee Member.

Xinkai Chen (M'96–SM'02) received the Ph.D. degree in engineering from Nagoya University, Nagoya, Japan, in 1999.

Currently, he is a Professor with the Department of Electronic and Information Systems, Shibaura Institute of Technology, Tokyo, Japan. His research interests include adaptive control, smart materials, hysteresis, sliding mode control, machine vision, and observer.

Dr. Chen has served as an Associate Editor of several journals, including the IEEE TRANSACTIONS ON AUTOMATIC CONTROL, IEEE TRANSACTIONS ON CONTROL SYSTEMS TECHNOLOGY, IEEE/ASME TRANSACTIONS ON MECHATRONICS, *European Journal of Control*, etc. He has also served for international conferences as Organizing Committee Member including Program Chairs, Program Co-Chairs, etc.

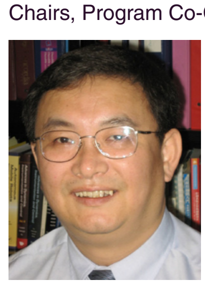

Chun-Yi Su (SM'99) received the Ph.D. degree in control engineering from the South China University of Technology, Guangzhou, China, in 1990.

He joined Concordia University, Montreal, QC, Canada, in 1998, after a 7-year stint with the University of Victoria, Victoria, BC, Canada. He is with the College of Mechanical Engineering and Automation, Huaqiao University, Quanzhou, China, on leave from Concordia University. He has authored or co-authored more than 300 publications in journals, book chapters, and conference proceedings. His research interests include application of automatic control theory to mechanical systems and control of systems involving hysteresis nonlinearities.

Dr. Su has served as an Associate Editor of the IEEE TRANSACTIONS ON AUTOMATIC CONTROL, IEEE TRANSACTIONS ON CONTROL SYSTEMS TECHNOLOGY, and the *Journal of Control Theory and Applications*. He has been on the Editorial Board of 18 journals, including the *IFAC Journal of Control Engineering Practice and Mechatronics*. He served for many conferences as an Organizing Committee Member. He was the recipient of several Best Conference Paper Awards.